Degradation of Oxidized Insulin B Chain by the Multiproteinase Complex Macropain (Proteasome)†

Lawrence R. Dick,‡ Carolyn R. Moomaw,§ George N. DeMartino,‖ and Clive A. Slaughter*,‡,§

Departments of Biochemistry and Physiology and Howard Hughes Medical Institute, The University of Texas Southwestern Medical Center, 5323 Harry Hines Boulevard, Dallas, Texas 75235

Received October 1, 1990; Revised Manuscript Received December 14, 1990

ABSTRACT: The peptides generated from the degradation of the oxidized B chain of bovine insulin by the multiproteinase complex macropain (proteasome) have been analyzed by reverse-phase peptide mapping and identified by N-terminal amino acid sequencing and composition analysis. Six of the 29 peptide bonds in the insulin B chain were found to be rapidly cleaved by macropain. The catalytic center that cleaves the Gln_4–His_5 bond could be distinguished from the center or centers that cleave the other preferred bonds by its specific susceptibility to inhibition by leupeptin, antipain, chymostatin, and pentamidine, suggesting that macropain utilizes at least two distinct catalytic centers for the degradation of this model polypeptide. The same effectors simultaneously enhance the rate of cleavage at the other susceptible sites in insulin B. The quantitative characteristics of this effect indicate that different catalytic centers of the complex may be functionally coupled, possibly by an allosteric mechanism or possibly by a mechanism in which binding to the catalytic centers is preceded by a rate-limiting binding of the substrate to a site or sites on the enzyme distinct from the catalytic centers. The kinetics of insulin B chain degradation indicate that macropain can catalyze sequential hydrolysis of peptide bonds in a single substrate molecule via a reaction pathway that involves channeling of peptide intermediates between different catalytic centers within the multienzyme complex. This capacity for channeling may confer potential physiological advantages of increasing the efficiency of amino acid recycling and reducing the pool sizes of peptide intermediates that are generated during the degradation of polypeptides in the intracellular milieu.

The high molecular weight proteinase macropain has been isolated from numerous tissues and from a broad range of eukaryotic organisms (Rivett, 1989a) and is thought to function in the nonlysosomal pathways of intracellular protein degradation (McGuire & DeMartino, 1989). The enzyme has an estimated molecular weight of 650 000 and is composed of several small polypeptide subunits with molecular weights in the range of 21 000–35 000 (McGuire & DeMartino, 1986). The subunits represent the products of at least 13 different genes encoding polypeptides of different amino acid sequences (Lee et al., 1990). These subunits are noncovalently associated in an unknown stoichiometry to form a complex with a cylindrical morphology (Baumeister et al., 1988).

It has been proposed that different macropain subunits contain proteolytic active centers with different substrate specificities (Wilk & Orlowski, 1983) and thus that macropain is a multienzyme complex. Although this hypothesis has been generally accepted, there remains disagreement as to the number of distinct catalytic centers, the substrate specificity of the catalytic centers, and the mechanistic class or classes to which the proteolytic activities belong (Mason, 1990; Orlowski & Michaud, 1989; Rivett, 1989b). Specific catalytic functions of the enzyme have not yet been assigned to particular subunits of the complex. Furthermore, the role of the different catalytic centers in the degradation of polypeptides, as distinct from their role in the degradation of low molecular weight substrates and short peptides, remains largely unexplored.

The work presented here provides a description of the way in which macropain degrades a model polypeptide substrate, the oxidized B chain of bovine insulin (insulin B_{ox}).[1] The effects of proteinase inhibitors and the kinetics of the degradation are presented. The data indicate that at least two distinct types of catalytic center in the complex are involved in the degradation of this substrate. Furthermore, the data suggest that the enzyme can degrade polypeptides processively, by channeling intermediates from one catalytic center to another.

Materials and Methods

Purification of Latent Macropain from Human Erythrocytes. Macropain in the latent form was purified from outdated human red cells essentially as described (McGuire et al., 1989) with the following modifications. Red blood cells were lysed in a buffer of 5 mM Tris-HCl, pH 7.2, and 5 mM 2-mercaptoethanol. Batch and column ion-exchange separations and gel-filtration chromatography were performed in 20 mM Tris-HCl, pH 7.2, 20 mM NaCl, 0.5 mM dithiothreitol (DTT), and 10% (v/v) glycerol (buffer A). Throughout the procedure, macropain was identified by assaying for hydrolysis of Z-Val-Leu-Arg-MNA as described (McGuire & DeMar-

† This work was supported by the American Heart Association Texas Affiliate Inc. (89G-074).

* To whom correspondence should be addressed at Howard Hughes Medical Institute, The University of Texas Southwestern Medical Center, 5323 Harry Hines Blvd, Dallas, TX 75235.

‡ Department of Biochemistry.

§ Howard Hughes Medical Institute.

‖ Department of Physiology.

[1] Abbreviations: insulin B_{ox}, oxidized B chain of bovine insulin; Tris, tris(hydroxymethyl)aminomethane; DTT, dithiothreitol; Z, benzyloxycarbonyl; MNA, 4-methoxy-2-naphthylamine; SDS–PAGE, sodium dodecyl sulfate–polyacrylamide gel electrophoresis; HPLC, high-performance liquid chromatography; TFA, trifluoroacetic acid; PTH, phenylthiohydantoin; PTC, phenylthiocarbamyl; 2NA, 2-naphthylamine; Cys(SO_3^-), cysteic acid residue; tBoc, *tert*-butyloxycarbonyl; AMC, 7-amino-4-methylcoumarin; pNA, *p*-nitroanilide; Bz, benzyl; Suc, succinyl.

0006-2960/91/0430-2725$02.50/0

tino, 1986). After the initial fractionation of the erythrocyte lysate by ion exchange and gel filtration on Sephacryl S300, the active material was applied to a 1.5 × 25 cm column of heparin–agarose equilibrated with buffer A, and bound protein was eluted with a 200-mL linear gradient of 20–300 mM NaCl. The active material was dialyzed against buffer containing 25 mM sodium phosphate, pH 6.8, 20 mM NaCl, 0.5 mM DTT, 10 μM $CaCl_2$, and 10% (v/v) glycerol and applied to a 1.5 × 6 cm column of hydroxylapatite equilibrated in the phosphate buffer at room temperature. The protein was eluted with a 200-mL linear gradient of 25–400 mM sodium phosphate. The purity of the active fractions was assessed by SDS–PAGE. Silver staining with prolonged color development revealed the known components of macropain (21–35 kDa) as the only polypeptides present in significant quantity. Other polypeptides detected in some preparations individually accounted for less than 1% of the total protein. Protein concentrations measured by the method of Bradford (1976) with bovine serum albumin as a standard indicated that 25 mg of latent macropain was typically obtained from 1.5 L of packed red blood cells. The enzyme was stored at −20 °C in buffer A, at a protein concentration of 0.5–1.0 mg/mL.

Preparation of Insulin B_{ox} Substrate. Insulin B_{ox} (50 mg; Sigma Chemical Co., St. Louis, MO) was mixed with 5 mL of water, and 25 μL of 1 N NaOH was added to dissolve the peptide. The pH of the stock solution was 8.5 and the concentration was $(2.6 \pm 0.2) \times 10^{-3}$ M as determined by amino acid analysis as described below. This concentration value was in good agreement with the manufacturer's specifications. For some experiments the stock solutions of insulin B_{ox} were repurified by high-performance liquid chromatography (HPLC), as described below, by isocratic elution with a solution containing 74% (v/v) water, 26% (v/v) acetonitrile, and 0.01% (v/v) trifluoroacetic acid (TFA). The major peak of eluting material detected by absorption at 280 nm was collected and lyophilized. The powder was dissolved in water to provide a concentration of $(1.9 \pm 0.1) \times 10^{-4}$ M as determined by amino acid analysis.

Digestion of Insulin B_{ox}. Prior to assay, 1 mL of latent macropain was thawed and dialyzed against 1 L of 10 mM Tris-HCl, pH 7.2, and 0.5 mM DTT buffer for 2–3 h at room temperature to activate the proteinase activity. Insulin B_{ox} was digested at 37 °C in 40 mM Tris-HCl, pH 8.0, and 1 mM DTT buffer. The concentration of enzyme and substrate and the time of digestion were varied as indicated in the figure legends. Digestion was stopped at the indicated times by addition of TFA to provide a final concentration of 0.2% (v/v).

N-Terminal Amino Acid Sequencing and Amino Acid Analysis. Peptides were subjected to automated Edman degradation on a Model 470A amino acid sequencer (Applied Biosystems, Inc., Foster City, CA) equipped with a Model 120A PTH-amino acid analyzer, using standard manufacturer's programming and chemicals. The concentrations of peptides were measured by quantitative amino acid analysis with the Waters Pico-Tag system. Amino acid calibration standards were obtained from Pierce Chemical Company (Rockford, IL). Each amino acid analysis was performed on three replicate samples. Standard deviations of the amounts of individual phenylthiocarbamyl- (PTC-) amino acids ranged from 2 to 5%. Peptide concentrations, were calculated by using the mean quantity of each PTC amino acid detected, multiplied by the appropriate dilution factor. Standard deviations for three determinations ranged from 5 to 8%.

Chromatographic Analysis of Insulin B_{ox} Digests. Liquid chromatography was performed on an HPLC system from the Waters Chromatography Division of Millipore (Milford, MA), with a 4.6 × 250 mm RP-300 column from Applied Biosystems, Inc. Typically, 1.8–6.4 nmol of digest in an injection volume of 40–115 μL was used for each chromatographic analysis. Chromatography was performed at 40 °C in 0.01% (v/v) TFA in water at a flow rate of 0.5 mL/min. Elution was performed with a 120-min linear gradient of 0–60% (v/v) acetonitrile with 0.01% (v/v) TFA, begun 10 min after injection. The absorbance was monitored at 214 nm and the results of the analyses were digitized, stored, and integrated by using a Waters Model 840 chromatography data station. In order to calibrate the HPLC assay for purposes of quantitation, a large-scale isolation of insulin B_{ox} digestion products was first performed. A 1-mL aliquot containing 200 nmol of insulin B_{ox} digest was injected onto the column and the component peptides were collected manually and lyophilized. Each peptide was redissolved in 100 μL of 1 mM ammonium hydroxide and then the solutions were neutralized by addition of 100 μL of 1 mM acetic acid. Two of the peptides, peptide (18–30)[2] and peptide (14–30), were not readily solubilized by this procedure but could be dissolved in dimethyl sulfoxide. The concentrations of the resulting peptide solutions were measured by amino acid analysis and were typically in the range of $(0.5–2.0) \times 10^{-4}$ M. Serial dilutions of peptide stock solutions were made in assay buffer containing 0.2% TFA. These samples were subjected to chromatography under conditions identical with those used for analysis of digests. The peak areas were plotted against the amount of peptide injected into the column to generate calibration curves, with which unknown quantities could be measured by interpolation. The plots for peptides (1–4), (5–13), (20–30), (1–13), and (18–30) gave straight lines over the entire range of peak areas encountered in the unknown samples. Linear regression of peak area on amount of peptide injected yielded correlation coefficients of 1.00 for each of these peptides, and the lines extrapolated close to $x = 0$, $y = 0$ by the method of least squares. However, calibration data for peptides (14–30) and (5–30) and insulin B_{ox} showed pronounced concave curvature for quantities below 500 pmol injected. Furthermore, the peaks corresponding to peptide (5–30) and insulin B_{ox} also partially overlapped one another so that the peak area measured for each was influenced by the amount of the other. In order to quantitate these two peptides, peak areas for each were measured in the presence of different amounts of the other in order to derive empirical corrections that could be applied to the measurements. Finally, quantities of peptide (1–11) were estimated by using the same calibration curve as that used for peptide (1–13) because of the extensive similarity in their structures. The reproducibility of the HPLC assay was tested by making repeated injections of the same sample, by injecting different dilutions of a sample in the same injection volume, and by injecting different volumes of the sample. From the resulting data, the precision of the measurements was estimated to be ±2% over the range of interest. For the peptides studied, injections of 1 pmol yielded a readily detectable signal, but injections of 10 pmol or more were required to give reproducible peak areas. The error bars on the progress curves shown in the figures represent the standard deviations of values measured in three replicate digests. These error bars reflect the precision of the HPLC assay as well as the precision in mixing of and sampling from the digests.

[2] Peptide fragments of insulin B_{ox} are designated according to the positions that their N- and C-terminal residues occupy within the intact insulin B_{ox} polypeptide chain; e.g., peptide (18–30) identifies the fragment extending from the 18th to the 30th residue in insulin B_{ox}.

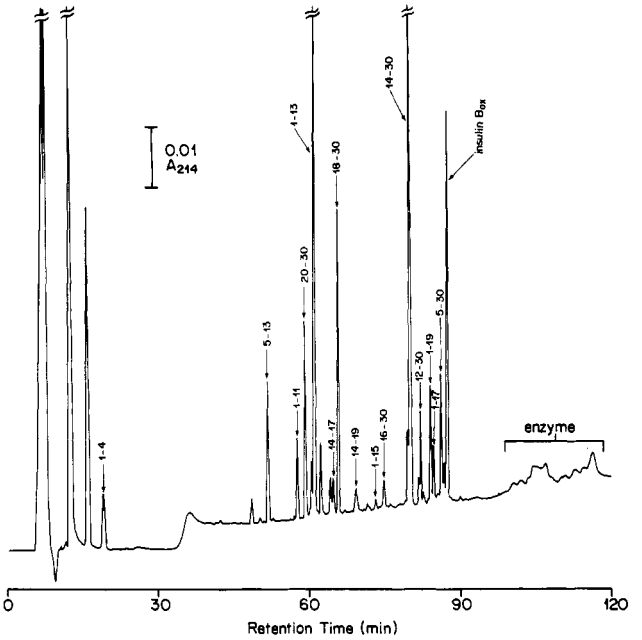

FIGURE 1: Reverse-phase chromatogram of the peptides generated during the degradation of insulin B_{ox} by dialysis-activated macropain. Insulin B_{ox} (2×10^{-5} M) was incubated with 6×10^{-8} M dialysis-activated macropain in a final volume of 1.1 mL for 35 min under standard conditions (see Materials and Methods). A 92-μL aliquot of the digest was subjected to chromatography. Approximately 85% of the initial amount of substrate has been consumed and the peak labeled insulin B_{ox} corresponds to the remaining 15%. Most of the peaks in the chromatogram correspond to fragments of insulin B_{ox} and these are designated by residue numbers, e.g., the peak labeled 1-4 corresponds to peptide (1-4), etc. The large peaks to the left of peptide (1-4) result from buffer components, predominantly Tris and DTT. The envelope of broad, overlapping peaks labeled enzyme corresponds to the subunits of macropain. The identities of unlabeled peaks have not yet been firmly established, but preliminary results suggest the following probable assignments. The peak that overlaps peptide (14-17) contains residues 20-28 of insulin B_{ox}. The unlabled peak immediately following peptide (1-13) represents a modified form of peptide (1-13) in which deamidation of Asn_3 or Gln_4 has occurred. The peak preceding peptide (5-13) at a retention time of 48 min corresponds to residues 1-7 of insulin B_{ox}.

RESULTS

Products of Degradation of Insulin B_{ox} by Activated Macropain. Several prominent peaks were resolved by high performance liquid chromatography of a sample of insulin B_{ox} that had been digested with human erythrocyte macropain (Figure 1). These peaks were absent in chromatograms of samples incubated either in the absence of the enzyme or in the absence of insulin B_{ox}, indicating that they corresponded to peptide fragments of insulin B_{ox} produced by enzymatic cleavage. The peptides were collected and identified by N-terminal amino acid sequencing and amino acid composition analysis. The results are summarized in Figure 1. Sequence alignment of the peptides with intact insulin B_{ox} indicated that their production minimally required cleavage of six different peptide bonds within the substrate (Figure 2). Five of these six bonds were also identified by Rivett (1985), using macropain from rat liver. However, chromatograms of insulin B_{ox} digested for prolonged periods (20 h or more, data not shown), were observed to contain several components in addition to those shown in Figure 1. N-terminal amino acid sequencing and amino acid composition analysis were used to identify the corresponding fragments, and eight additional sites of cleavage were inferred (Figure 2). Thus 14 of the 29 peptide bonds in insulin B_{ox} are susceptible to cleavage by macropain, of which six are more rapidly cleaved than the other eight.

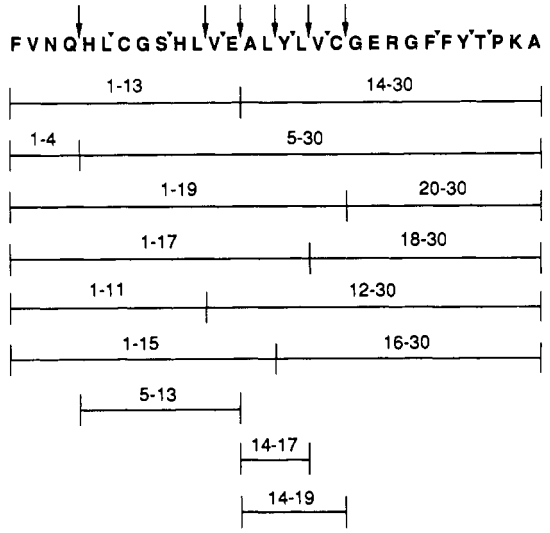

FIGURE 2: Positions of cleavage of insulin B_{ox} by macropain and the primary products generated. The amino acid sequence of insulin B_{ox} is shown with the conventional single-letter code: C is used to designate the oxidized form of cysteine, cysteic acid. The peptides that accumulate early in the course of digestion are shown below. The large arrows (↓) above the sequence indicate the location of the peptide bonds that are cleaved to generate the fragments observed early in digestion. The small arrows (▼) point to additional cleavage sites at which hydrolysis produced peptides that accumulate at later stages of digestion (see text).

The macropain used for digestion of insulin B_{ox} was isolated in a latent form that shows low specific activity for the degradation of casein to acid soluble peptides (Tanaka et al., 1986; McGuire et al., 1989). The latent enzyme was activated prior to use in the present study by removing glycerol and sodium chloride by dialysis. McGuire et al. (1989) have shown that this procedure increases the proteinase activity of the enzyme up to 50-fold while affecting certain peptidase activities relatively slightly. In the present study, degradation of insulin B_{ox} by dialysis-activated macropain was much more rapid than degradation by latent macropain. Thus the amounts of peptides (1-13) and (14-30) generated by latent macropain in short-term digests of less than 1 h were $\leq$3% of the amounts generated by the dialysis-activated enzyme. Even upon prolonged incubation with latent macropain (several hours), little insulin B_{ox} degradation was observed. The results with insulin, a 30-residue polypeptide, therefore closely mimic those with the protein substrate, casein, indicating that insulin B_{ox} is an appropriate model substrate for the degradation of proteins.

Six independently isolated preparations of macropain were used over the course of the present study. Digestion of insulin B_{ox} always yielded the same peptide fragments (Figures 1 and 2) and the relative quantities of all but two of the peptides were reproducible. The two fragments that exhibited some quantitative variation were peptides (1-15) and (16-30), both of which were produced in low abundance. The variability occurred both when different enzyme preparations were used and when different aliquots of the same enzyme preparation were used on different days (data not shown). The magnitude of the variation was approximately 2-fold. Figure 1 shows an example of a digest in which the quantity of these fragments was at the low end of the range. Since both peptides (1-15) and (16-30) can be produced by cleavage of insulin B_{ox} at a single site, Leu_{15}-Tyr_{16}, the variability in the accumulation of these two fragments reflects variability of a single enzymic activity. This activity also exhibited other unusual properties. Mersalyl acid (100 μM) failed to inhibit the accumulation of peptides (1-15) and (16-30), although it effected nearly

Table I: Potency of Proteinase Inhibitors in Preventing Macropain-Catalyzed Cleavage of Gln_4–His_5 in Insulin B_{ox}

inhibitor	$[I]_{0.5}$[a] (μM)
leupeptin	2
antipain	8
chymostatin	50
pentamidine	150
benzamidine	>1000[b]

[a] $[I]_{0.5}$ is defined as the inhibitor concentration required to effect a 50% decrease in the rate of accumulation of peptide (1–4). The enzyme was incubated with the inhibitor for 20 min prior to addition of substrate. [b] Benzamidine showed no inhibitory effect at 1000 μM, which was the highest concentration tested.

complete inhibition of all other activities. Moreover, these two peptides were generated in similar amounts by latent and by dialysis-activated macropain. These observations suggest that the cleavage of Leu_{15}–Tyr_{16} takes place in a catalytic center distinct from the catalytic center(s) responsible for cleavage at the other sites in insulin B_{ox}. Although the products of cleavage by this center were formed in relatively high abundance in the studies of Rivett (1985), they were of minor abundance in the present work.

Effect of Proteinase Inhibitors on the Degradation of Insulin B_{ox}. To test the hypothesis that different cleavages of insulin B_{ox} were being catalyzed in different catalytic centers of macropain, several compounds known to be competitive inhibitors of other proteolytic enzymes were tested for their effects on digestion of insulin B_{ox}. Four of these compounds, leupeptin, antipain, chymostatin, and pentamidine, yielded qualitatively similar results, which are illustrated in Figure 3 by data obtained with leupeptin. Peptides (1–4), (5–13), and (5–30) were much reduced or absent in mixtures containing leupeptin, antipain, chymostatin, or pentamidine. The production of each of these fragments requires cleavage at the Gln_4–His_5 bond, suggesting that cleavage of Gln_4–His_5 occurs in a catalytic center distinguished from the catalytic center or centers that cleave at the other sites in insulin B_{ox} by its susceptibility to inhibition by these four effectors.

As shown in Table I, leupeptin was the most potent of the four effectors. The $[I]_{0.5}$ value (defined in Table I) for leupeptin, 2 μM, is 100-fold lower than the substrate concentration used in the assays (Figure 4), suggesting that the affinity of macropain for leupeptin is at least 100 times greater than the affinity for insulin B_{ox}. Likewise, the apparent affinity of macropain for leupeptin is greater than that for the peptide substrates tBoc-Leu-Ser-Thr-Arg-AMC (K_M = 180 μM; Rivett, 1989b) and Z-Ala-Ala-Arg-MNA (K_M = 130 μM; Arribas & Castaño, 1990), although the apparent affinity for the peptide substrate Z-Val-Leu-Arg-MNA (K_M = 5 μM; L. R. Dick, unpublished observations) is of comparable magnitude. Mason (1990) has reported that leupeptin shows slow binding behavior with an association rate constant of 1290 s^{-1} M^{-1} and a K_i of 25 nM with preparations of human liver macropain. In the present study, however, when insulin B_{ox} was subjected to digestion by macropain following varying times of preincubation with 1 μM leupeptin, no evidence for slow binding was observed (data not shown). The $[I]_{0.5}$ value for pentamidine was 150 μM, but for reasons that are not yet clear the compound benzamidine, which consists of a structural motif that is represented in two covalently joined copies in pentamidine, failed to inhibit cleavage of the Gln_4–His_5 bond even at 1 mM concentration.

In addition to their inhibitory effects on the cleavage of the Gln_4–His_5 bond, the four effectors exercised a stimulatory effect on the cleavage at other sites in insulin B_{ox}. This can be seen in Figure 3B, where the product peaks, with the exception of the three that were suppressed, were larger than their counterparts in control digests (Figure 3A). Figure 4A shows how the magnitudes of the inhibitory and stimulatory effects depend upon leupeptin concentration in the range 1–10 μM at an early stage in the degradation of insulin B_{ox} (<35% of the substrate consumed). For all the products, the concentration required to produce 50% of the maximal observed inhibitory or stimulatory effect accords well with the $[I]_{0.5}$ value (2 μM) for the production of peptide (1–4) that is quoted as an example in Table I. These results are consistent with the simplest hypothesis for effector action under which both the inhibitory and the stimulatory effects are caused by the binding of leupeptin to a single site on macropain. Alternatively, leupeptin may be binding to two or more sites that have similar binding affinities. Similar results to those obtained with leupeptin were observed with the other two peptide aldehyde inhibitors, antipain and chymostatin (data now shown), but pentamidine yielded a significantly different result at concentrations below 40 μM, as shown in Figure 4B. The stimulatory effects were more pronounced than the inhibitory effects even at the early stage of degradation represented in Figure 4B, suggesting that there may be distinct "stimulatory" and "inhibitory" binding sites for this effector. Under the

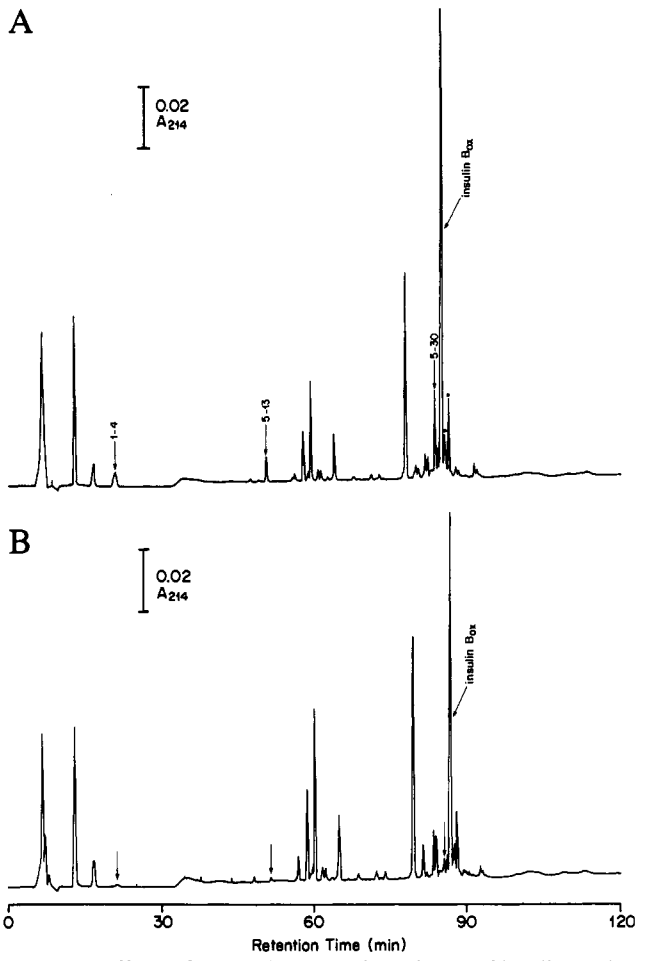

FIGURE 3: Effects of leupeptin on the degradation of insulin B_{ox} by macropain. Reverse-phase chromatograms of the peptides generated by digestion of 1×10^{-4} M insulin B_{ox} by 1.5×10^{-7} M dialysis-activated macropain in a final volume of 200 μL for 20 min in the absence (A) or presence (B) of 1×10^{-5} M leupeptin. Aliquots (32 μL) of the digests were subjected to chromatography. Approximately 30–40% of the initial amount of insulin B_{ox} remained intact at this time. The peaks marked with asterisks (*) in panel A are contaminants present in the substrate preparation as supplied by the manufacturer. For subsequent work (also for Figure 1) they were removed as described under Materials and Methods.

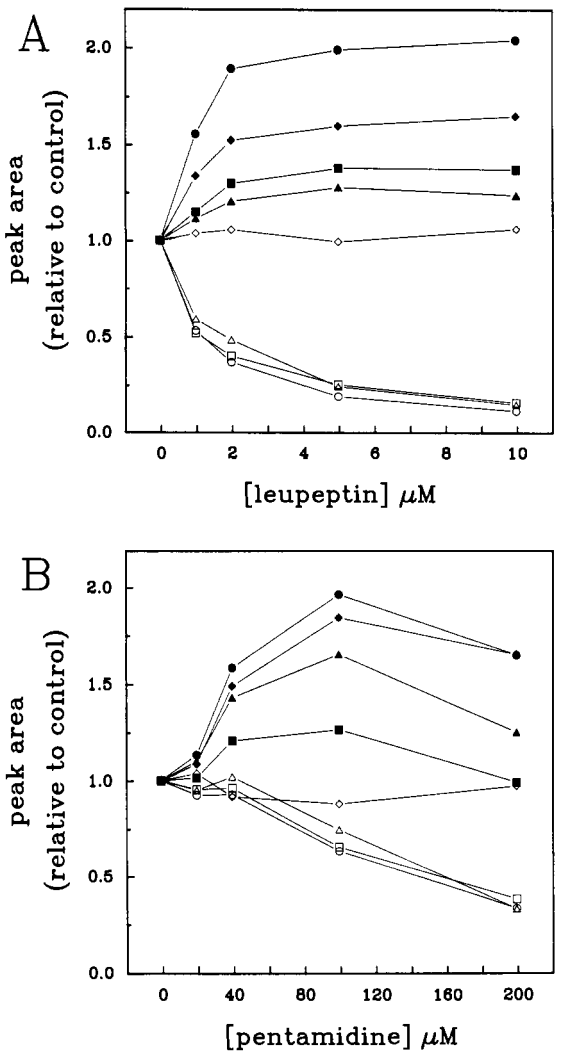

FIGURE 4: Quantitative effects of leupeptin (A) and pentamidine (B) on the accumulation of fragments of insulin B_{ox}. Digests containing 2×10^{-4} M insulin B_{ox} and 1.5×10^{-7} M dialysis-activated macropain were incubated in a final volume of 200 μL for 20 min (A) or 10 min (B) in the presence of inhibitors at various concentrations, and 32 μL of the digest was analyzed by HPLC. Velocities of product accumulation relative to the velocities in the absence of effector are shown as a function of effector concentration. The ordinate values were derived by dividing the integrated intensities of peaks in the chromatograms of samples containing effector by the integrated intensities of their counterparts in the chromatogram of a digest in the absence of the effectors. ◇, insulin B_{ox}; ○, peptide (1–4); △, peptide (5–13); □, peptide (5–30); ◆, peptide (20–30); ●, peptide (1–13); ▲, peptide (14–30); ■, peptide (18–30).

conditions illustrated in Figure 4A, the rate of depletion of insulin B_{ox} in the presence of leupeptin was independent of leupeptin concentration, indicating that the inhibitory and stimulatory effects on the consumption of insulin B_{ox} compensated for one another. It is noteworthy that, under such conditions, consideration of the data pertaining to substrate depletion without also considering the effects on the accumulation of individual products might have led to the erroneous conclusion that leupeptin has no effect on the degradation of insulin B_{ox}. At late stages of degradation, such as the stage illustrated in Figure 3 (>65% of the substrate consumed), the total depletion of insulin B_{ox} was greater in the presence of leupeptin than in controls, as can be seen by comparing the height of the insulin B_{ox} peak in the presence and absence of the effector in Figure 3. Under conditions such as these, if data on consumption of substrate were the only results available, it might have been erroneously concluded that leupeptin was behaving only as an activator and had no inhibitory effects. Furthermore, at higher concentrations of leupeptin (20–100 μM), panspecific suppression of the stimulatory effects was observed (data not shown), indicating that a broad range of effector concentrations must be tested in order to determine the range of effector influences. These various results indicate that interpreting the role of modifiers of the proteolytic activity of macropain measured by the consumption of acid-precipitable substrate proteins must be undertaken with caution.

Kinetics of Macropain Degradation of Insulin B_{ox}. When insulin B_{ox}, at a starting concentration of 2×10^{-5} M, was degraded by macropain, the disappearance of insulin B_{ox} behaved as a pseudo-first-order process (Figure 5A), suggesting that this substrate concentration is well below the saturating level. The first-order rate constant, k_{obs}, was 0.059 min^{-1}. The initial velocities of product accumulation were measured as a function of insulin B_{ox} concentration, and the values for $[S]_{0.5}$ [the apparent K_M (Atkinson, 1977)] for the different cleavages were estimated by using Eadie–Scatchard plots (data not shown). The values fell in the range of $(1–2) \times 10^{-4}$ M. By using a value of 650 000 for the molecular weight of a macropain particle, it may be estimated that the average velocity of insulin B_{ox} degradation during the first 5 min of this experiment (Figure 5A) was 14 molecules of insulin B_{ox} cleaved per minute per macropain particle. Extrapolating to saturating substrate concentration, the turnover number, k_{cat}, was ≥100 min^{-1}. Since there are apparently two or more different kinds of catalytic center in each particle and there may be more than one copy of a single kind of catalytic center in each particle, this turnover number presumably represents the sum of several independent contributions.

As shown in Figure 2, 12 of the 15 fragments of insulin B_{ox} that arise by cleavage at the six preferred sites may be grouped into complementary pairs, the members of which represent the products of single cleavages of the intact substrate. The remaining three of the 15 fragments each arise through the cleavage of insulin B_{ox} at a minimum of two sites. Although these various products may be derived from pathways in which insulin B_{ox} is cleaved in the minimum possible number of positions, they may be formed in more complex, multistep pathways. In order to establish the nature of the dominant pathways by which macropain degrades insulin B_{ox}, the simplest system of reactions that accounts for all the observed cleavage products was formulated as a model to be tested against experimental measurements of product accumulation. The model includes six parallel, first-order reactions that represent cleavages of intact insulin B_{ox} at the six preferred sites:

$$\text{insulin } B_{ox} \xrightarrow{k_1} (1–13) + (14–30) \quad (1)$$

$$\text{insulin } B_{ox} \xrightarrow{k_2} (1–4) + (5–30) \quad (2)$$

$$\text{insulin } B_{ox} \xrightarrow{k_3} (1–17) + (18–30) \quad (3)$$

$$\text{insulin } B_{ox} \xrightarrow{k_4} (1–19) + (20–30) \quad (4)$$

$$\text{insulin } B_{ox} \xrightarrow{k_5} (1–11) + (12–30) \quad (5)$$

$$\text{insulin } B_{ox} \xrightarrow{k_6} (1–15) + (16–30) \quad (6)$$

Each of these reactions is associated with a rate constant, k_1–k_6. The remaining three fragments, peptides (5–13), (14–17), and (14–19), arise through pathways that minimally consist of two consecutive cleavages, of which the first rep-

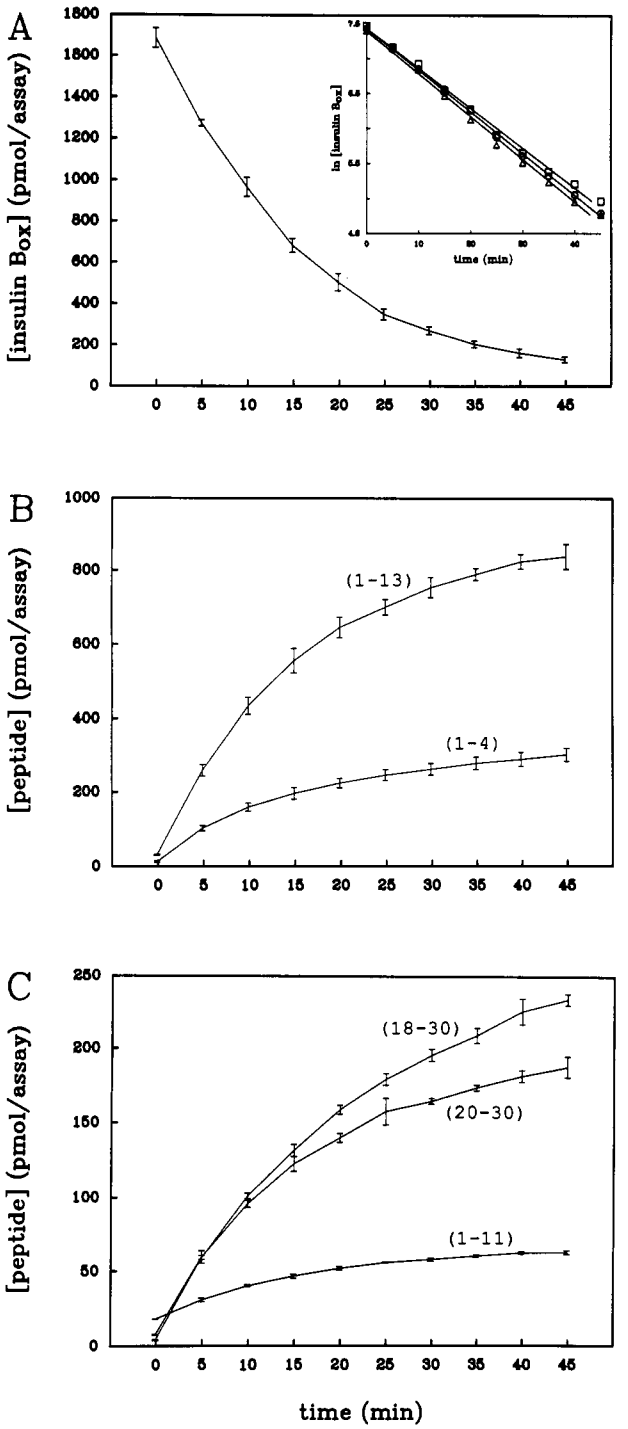

FIGURE 5: Progress curves for disappearance of substrate and accumulation of selected products of macropain-catalyzed degradation of insulin B_{ox}: apparent conformity to model of parallel, first-order, single-cleavage reactions. Insulin B_{ox} (2×10^{-5} M) was incubated with 6×10^{-8} M dialysis-activated macropain in a total volume of 1.1 mL under standard conditions. At 5-min intervals, 100-μL aliquots of the mixture were removed and acidified with TFA to stop digestion. The samples were analyzed by HPLC and the concentrations of the peptides were derived from the data by using the calibrations described under Materials and Methods. Panel A shows the progress curve for disappearance of insulin B_{ox}. The error bars give the standard deviations for three replicate digests. The chromatogram in Figure 1 represents one of the three 35-min time points shown here. A linear regression of the natural logarithm of insulin B_{ox} concentration on time of digestion was calculated for each of the three experiments (inset, panel A) and the slopes of the least-squares lines were averaged, yielding a pseudo-first-order rate constant, k_{obs}, for insulin B_{ox} disappearance of 0.059 ± 0.002 min^{-1}. Panels B and C show the progress curves for accumulation of peptides generated by reactions 1–5. Note the differences in the ordinate scales used in the three panels.

resents one of the reactions 1–6 above. Each of these three products may be formed by two alternative pathways, either or both of which may contribute toward its accumulation. Thus peptide (5–13) may be formed in the following two reactions:

$$(1\text{–}13) \rightarrow (1\text{–}4) + (5\text{–}13) \quad (7)$$

and

$$(5\text{–}30) \rightarrow (5\text{–}13) + (14\text{–}30) \quad (8)$$

where peptides (1–13) and (5–30) are intermediates generated in reactions 1 and 2, respectively. Peptide (14–17) may be formed in the following two reactions:

$$(14\text{–}30) \rightarrow (14\text{–}17) + (18\text{–}30) \quad (9)$$

and

$$(1\text{–}17) \rightarrow (1\text{–}13) + (14\text{–}17) \quad (10)$$

where peptides (14–30) and (1–17) are intermediates generated in reactions 1 and 3, respectively. Peptide (14–19) may be formed in the following two reactions:

$$(1\text{–}19) \rightarrow (1\text{–}13) + (14\text{–}19) \quad (11)$$

and

$$(14\text{–}30) \rightarrow (14\text{–}19) + (20\text{–}30) \quad (12)$$

where peptides (1–19) and (14–30) are generated in reactions 4 and 1, respectively. It may be noted that peptide (1–4) may be produced in reactions 2 and 7, peptide (18–30) in reactions 3 and 9, peptide (1–13) in reactions 1, 10, and 11, and peptide (20–30) in reactions 4 and 12.

The quantitative contributions of these pathways to the degradation of insulin B_{ox} were investigated by measuring the time course for the accumulation of selected products. The data are summarized in Table II and in Figures 5–7. The relative contributions of the six parallel, single-step reactions were first estimated by determining values for the apparent first-order rate constants, k_1–k_5, during the early stages of digestion. At such early times, the contributions of multistep pathways involving intermediates in free solution are expected to be small. k_6 was not determined because preliminary estimates suggested that the abundance of the products derived from the reaction was small compared to the products of reactions 1–5. An expression for the rate constant, k_n, for the nth reaction was derived from a consideration of the behavior of systems of parallel, first-order reactions, reviewed by Frost and Pearson (1961). It is expected that the rate of disappearance of insulin B_{ox} will be equal to the sum of the rates of reactions 1–6 and that the overall rate constant, k_{obs}, will be given by the sum of the rate constants k_1–k_6. Further, the concentrations of the products of these reactions will remain in constant ratio during the progress of digestion. For example, for reactions 1 and 2

$$[P_1]/[P_2] = k_1/k_2 \quad (13)$$

where $[P_1]$ represents the concentration of either of the two products of reaction 1 and $[P_2]$ represents the concentration of either of the products of reaction 2. Moreover, the condition of conservation of mass requires that

$$[\text{insulin } B_{ox}]_0 - [\text{insulin } B_{ox}]_t = \sum_{n=1}^{6} [P_n]_t \quad (14)$$

where $[\text{insulin } B_{ox}]_0$ and $[\text{insulin } B_{ox}]_t$ represent the initial concentrations of insulin B_{ox} and the concentration after time t, respectively, and $[P_n]_t$ represents the concentration of either of the products of the nth reaction after time t. Combination

Table II: Relative Specificity of Macropain for Cleavage of Different Sites in Insulin B_{ox}

reaction	peptide bond cleaved	products[a]	k_n/k_{obs}[b]
1	Glu_{13}–Ala_{14}	*(1–13)* + (14–30)	0.52 ± 0.05
2	Gln_4–His_5	*(1–4)* + (5–30)	0.20 ± 0.01
3	Leu_{17}–Val_{18}	(1–17) + *(18–30)*	0.12 ± 0.01
4	$Cys(SO_3^-)_{19}$–Gly_{20}	(1–19) + *(20–30)*	0.12 ± 0.01
5	Leu_{11}–Val_{12}	*(1–11)* + (12–30)	0.05 ± 0.01
6	Leu_{15}–Tyr_{16}	(1–15) + (16–30)	nd
total			1.01 ± 0.09

[a] Values for k_n/k_{obs} were calculated by using data from the products shown in italic type. [b] k_n/k_{obs} values were calculated by using eq 15, and they represent the mean ± SD of three measurements taken at each of two time points, 5 and 10 min.

of these various relationships yields the following expression for k_n:

$$[P_n]_t/([\text{insulin } B_{ox}]_0 - [\text{insulin } B_{ox}]_t) = k_n/k_{obs} \quad (15)$$

Figure 5B,C shows progress curves for single products from reactions 1–5, including peptide (1–13) from reaction 1, peptide (1–4) from reaction 2, peptide (18–30) from reaction 3, peptide (20–30) from reaction 4, and peptide (1–11) from reaction 5. By using eq 15 in conjunction with the data in these progress curves, the rate constants for the individual reactions were calculated on the basis of the accumulation of products during the earliest stages of digestion (5- and 10-min time points only). The resulting values are shown in Table II. The data indicate that cleavage of the Glu_{13}–Ala_{14} bond is responsible for 52% of the insulin B_{ox} degraded, cleavage of the Gln_4–His_5 bond is responsible for 20%, cleavage of the Leu_{17}–Val_{18} bond and the $Cys(SO_3^-)_{19}$–Gly_{20} bond are responsible for 12% each, and cleavage of the Leu_{11}–Val_{12} bond is responsible for 5%.

The shapes of the progress curves for product accumulation were next analyzed by fitting them to the model of reactions 1–6, assuming that none of the products is subjected to further degradation. A general property of a system of parallel first-order reactions proceeding from a common substate (e.g., reactions 1–6) is that the shapes of the progress curves for product accumulation should all conform to the exponential decay of the substrate. Thus, a plot of product accumulation vs $1 - e^{-k_{obs}t}$ should be a straight line, provided that the product comes only from reactions 1–6 and is not turned over. Deviations from this behavior provide evidence of additional reactions, e.g. reactions (7) – (12), operating in the system. Figure 6C illustrates such plots for three of the peptides, peptides (1–13) and (14–30) from reaction 1 and peptide (18–30) from reaction 3. The plot for peptide (1–13) yielded a reasonably straight line, indicating that the progress curve for this peptide fits the simple model. Similar plots for peptide (1–4) from reaction 2, peptide (20–30) from reaction 4, and peptide (1–11) from reaction 5 also yielded straight lines (data not shown). However, the plot for peptide (14–30) from reaction 1 showed a convex curvature, suggesting that this fragment is turned over. This result is consistent with the operation or reactions 9 and 12 above. Conversely, the plot for peptide (18–30) from reaction 3 showed concave curvature, suggesting that this peptide is produced by some reaction in addition to reaction 3, presumably reaction 9. As shown in Figure 6A,B, evidence for turnover can also be seen at later stages of digestion in the progress curves for peptide (5–30) from reaction 2, peptide (1–17) from reaction 3, and peptide (1–19) from reaction 4. In these curves, the concentration of the product rises to a maximum value, then slowly falls owing to consumption by secondary cleavage(s). These results are consistent with the operation of reactions 8, 10, and 11, respectively. These analyses thus provide supplementary evidence for the operation of cleavage reactions 8–12 as predicted in the overall model for the degradation of insulin B_{ox}. The failure to detect the action of reaction 7 in the progress curve for peptide (1–13) may be due to the maintenance of a balance between the consumption of peptide (1–13) in reaction 7 and its supplemental production in reactions 10 and 11.

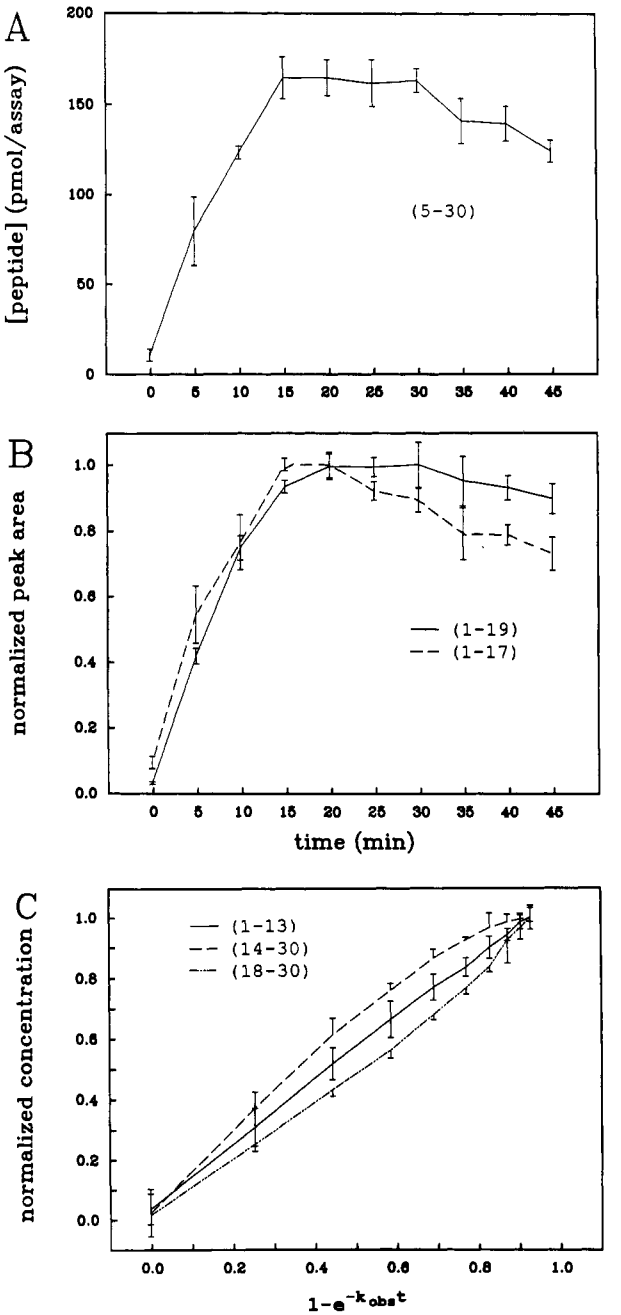

FIGURE 6: Deviations from the model of parallel, first-order, single-cleavage reactions. (A) Progress curve for peptide (5–30). (B) Progress curves for peptides (1–17) and (1–19). All three peptides show a fall in concentration at later stages of digestion. The ordinate values in panel B are the integrated intensities of the corresponding peaks divided by the maximum values observed during the time course of the experiment. The data come from the same experiment as the one shown in Figure 5. (C) Accumulation of peptides (1–13), (14–30), and (18–30) plotted on the relative time scale of insulin B_{ox} disappearance, $1 - e^{-k_{obs}t}$. The curvature observed in the plots for peptides (14–30) and (18–30) indicates that the accumulation of these two peptides deviates from expectations based on the model of parallel, single-cleavage reactions.

In order to test the hypothesis that the products requiring at least two cleavages within insulin B_{ox} are generated by

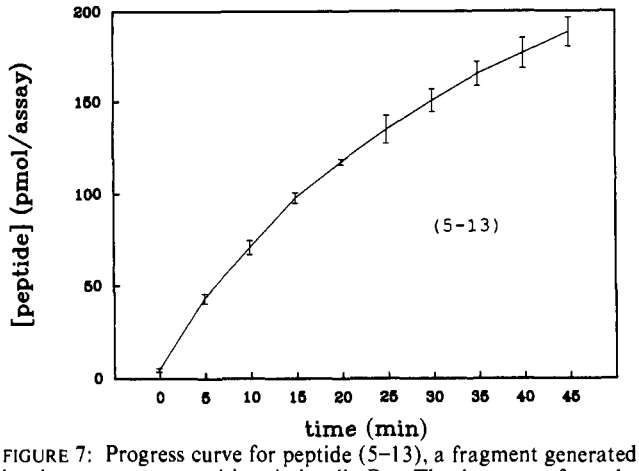

FIGURE 7: Progress curve for peptide (5–13), a fragment generated by cleavages at two positions in insulin B_{ox}. The data come from the experiment described in Figure 5.

consecutive reactions (eqs 7–12) as described above, the formation of one such product, peptide (5–13), was investigated in detail. As indicated above, this peptide is formed by the sum of two pathways, each consisting of a pair of consecutive reactions:

$$\text{insulin } B_{ox} \xrightarrow{k_1} (1\text{–}13) \rightarrow (1\text{–}4) + (5\text{–}13) \quad (16)$$

$$\text{insulin } B_{ox} \xrightarrow{k_2} (5\text{–}30) \rightarrow (5\text{–}13) + (14\text{–}30) \quad (17)$$

The relative contributions of these two pathways to the formation of peptide (5–13) are not known. The progress curve for the accumulation of peptide (5–13) is shown in Figure 7. The curve displays a maximal rate of accumulation during the earliest time interval, 0–5 min, and the rate decreases continuously throughout the course of digestion. The form of this curve, however, is inconsistent with the model as stated, because this model implies that the rate of accumulation of peptide (5–13) should exhibit a lag or induction period during which the concentrations of the intermediates, peptides (1–13) and (5–30), rise to their maximal values (Kuchel, 1985). The concentrations of peptides (1–13) and (5–30) reached maximum values at $t \geq 45$ min and $t \approx 15$ min, respectively (see Figures 5B and 6A). The absence of a comparable lag period in the accumulation of peptide (5–13) indicates that the intermediate concentrations being measured in free solution are not those that determine the rate of formation of the final product, peptide (5–13). This suggests that transfer or channeling of intermediates between the catalytic center that cleaves the Gln_4–His_5 bond and the center that cleaves the Glu_{13}–Ala_{14} bond occurs during degradation of insulin B_{ox} by macropain without release of the intermediate(s) from the enzyme surface into free solution.

The involvement of such channeling of intermediates complicates the interpretation of the values for k_n/k_{obs} in Table II. The use of these values as descriptors of the first-order rate constants for reactions 1–5 depends upon the assumption that secondary cleavage reactions contribute little to the rate of accumulation of the products at the earliest stages of digestion (see above). Although this is likely to be true for cleavages of intermediate products that are released from the enzyme into free solution, it is unlikely to be true for intermediates that are channeled to a second catalytic center and immediately cleaved a second time. In light of the involvement of channeling, k_n/k_{obs} may be reinterpreted as representing a rate constant for the total production of a fragment in the single-cleavage reaction plus the production of the same fragment in the relevant double-cleavage reactions that are mediated by channeling. However, the value for k_1/k_{obs} is an especially complicated case because its value is calculated on the basis of data for peptide (1–13), which may itself represent a channeled intermediate. In this case, only those cleavages of the Glu_{13}–Ala_{14} bond that produce an intermediate molecule of peptide (1–13) that is released into free solution are recognized. Those cleavages that produce a molecule that is channeled and immediately degraded are not observed. The value for k_1/k_{obs} thus excludes the contribution of cleavages of channeled molecules and represents only those cleavages derived from reaction 1. These considerations indicate that the ranking of the sites according to their relative frequency of cleavage early in the degradation of insulin B_{ox}, namely, Glu_{13}–Ala_{14} > Gln_4–His_5 > Leu_{17}–Val_{18} = $Cys(SO_3^-)_{19}$–Gly_{20} > Leu_{11}–Val_{12}, remains as indicated above.

Discussion

Identification and Specificity of Macropain Catalytic Centers That Degrade Insulin B_{ox}. It is of interest to inquire how the catalytic centers responsible for different cleavages of insulin B_{ox} correspond to the macropain activities that were defined in terms of specificity for synthetic peptide substrates by Wilk and Orlowski (1983). Of the three peptidase activities that were distinguished by these investigators, one was operationally defined by its ability to cleave D-Ala-Phe-Leu-Arg-2NA and Z-D-Ala-Leu-Arg-2NA and by its specific susceptibility to inhibition by leupeptin. Since cleavage of the Gln_4–His_5 peptide bond in insulin B_{ox} is also inhibited by leupeptin, it may be concluded that the catalytic center responsible for this cleavage is the same as that which cleaves D-Ala-Phe-Leu-Arg-2NA and Z-D-Ala-Leu-Arg-2NA. The $[I]_{0.5}$ value for the inhibition of the Gln_4–His_5 cleavage by leupeptin, 2 μM (see Table I), is in accord with the leupeptin K_i value of 1.3 μM reported by Wilk and Orlowski (1983) for inhibition of the cleavage of Z-D-Ala-Leu-Arg-2NA by bovine pituitary macropain and the leupeptin K_i value of 1 μM reported by Rivett (1989b) for inhibition of the cleavage of tBoc-Leu-Ser-Thr-Arg-AMC by rat liver macropain. Although the term "trypsinlike" has often been used to designate the leupeptin-inhibitable activity that hydrolyzes peptide substrates containing P1 arginyl residues, the present observation that this activity can also cleave the Gln_4–His_5 bond indicates that a P1 arginyl residue is not a necessary determinant of its specificity. Furthermore, since no evidence for cleavage at Arg_{22}–Gly_{23} in insulin B_{ox} has been obtained, a P1 arginyl residue may not be a sufficient determinant of specificity for this activity. The present observation that the chymotrypsin inhibitor chymostatin also inhibits cleavage of the Gln_4–His_5 bond is consistent with the findings of several investigators (Dahlmann et al., 1985a; McGuire and DeMartino, 1986; Tanaka et al., 1986; Zolfaghari et al., 1987; Folco et al., 1988; Saitoh et al., 1989; Rivett, 1989b; Mason, 1990) that chymostatin, as well as leupeptin, inhibits macropain-catalyzed cleavage of peptide substrates containing P1 arginyl residues. Chymostatin may also inhibit cleavage of substrates such as Suc-Leu-Leu-Val-Tyr-AMC that are mediated by a catalytic center(s) distinct from the trypsinlike center (Tanaka et al., 1988), but this inhibitor suppressed no other cleavage in insulin B_{ox} during the present study.

The other two activities originally defined by Wilk and Orlowski (1983) are, first, an activity defined by the hydrolysis of Z-Gly-Gly-Leu-pNA or Z-Gly-Arg-Leu-2NA that is specifically inhibited by Z-Gly-Gly-Leucinal, and, second, an activity defined by the hydrolysis of Z-Leu-Leu-Glu-2NA that is specifically stimulated by SDS. It appears, however, that

the particular choice of substrate may complicate the identification of these catalytic centers. For example, Orlowski and Michaud (1989) have shown that substrates containing a P1 phenylalanyl residue can be hydrolyzed in either of these two catalytic centers. Also, Tanaka et al. (1989), studying the activation of macropain by SDS, have demonstrated that identical profiles of activation as a function of SDS concentration are obtained with Suc-Leu-Leu-Val-Tyr-AMC and Z-Leu-Leu-Glu-2NA as substrates, suggesting that substrates with either aromatic or acidic amino acids at the P1 position may sometimes be cleaved in the same catalytic center. Thus, any assignment of the cleavages at Leu_{11}–Val_{12}, Glu_{13}–Ala_{14}, Leu_{17}–Val_{18}, or $Cys(SO_3^-)_{19}$–Gly_{20} to particular catalytic centers in macropain necessarily must be tentative. It is possible that a single type of catalytic center may be responsible for all of these cleavages. It may be noted that the site in insulin B_{ox} most commonly cleaved, Glu_{13}–Ala_{14}, contains a P1 glutamyl residue. The catalytic center responsible for this cleavage may be the same as the one that cleaves Z-Leu-Leu-Glu-2NA. It is interesting that the preferred site for the macropain-catalyzed cleavage of ribonuclease T_1 from *Aspergillus*, Glu_{28}–Asp_{29}, also has glutamic acid in the P1 position (L. R. Dick, C. N. Pace, et al., unpublished observations).

Action of Effector Molecules on Macropain. Work by others has shown that certain compounds stimulate the macropain-catalyzed cleavage of some substrates yet inhibit the cleavage of other substrates (Wilk & Orlowski, 1983; Dahlmann et al., 1985b; Orlowski & Michaud, 1989). The present study confirms and extends these findings by showing that cleavage at distinct sites within a single substrate molecule may be subject simultaneously to stimulation and inhibition by a single type of effector molecule. The present observations support the hypothesis that a substrate–enzyme–inhibitor ternary complex is formed and provide a basis for formulating and evaluating simple mechanistic models for the action of effectors. If both the inhibitory and stimulatory effects of leupeptin are exerted by binding of the effector to a single site or type of site, and if this site overlaps one of the catalytic centers (i.e., the inhibition is competitive), then two general models for the role of the effector molecule may be considered. The first is an allosteric model, in which binding of the effector to one catalytic center produces stimulation of another catalytic center by transmission of a conformational change to the latter. An interesting feature of this model, regarding the catalytic function of a multienzyme complex, is that the effector molecule may be mimicking an in vivo effector that plays a role in coordinate regulation of the different catalytic centers in the complex. In an alternative model, the effector molecule plays a passive role in the stimulation. Substrate first binds to the enzyme at a site that is distinct from any of the catalytic centers. The formation of the resulting complex precedes transfer of substrate to one or other of the catalytic centers for cleavage, as shown in Scheme IA. The enzyme, E, is represented as containing two catalytic centers, E_1 and E_2. The initial complex, in which substrate, S, is bound to a site distinct from E_1 and E_2 is represented by $S(E_1E_2)$, and the complexes in which S is bound to a catalytic center are represented by $E_1(E_2S)$ and $(E_1S)E_2$ respectively. It is assumed that the transfer of substrate from the initial binding site in $S(E_1E_2)$ to either of the two catalytic centers is rapid compared to dissociation of the $S(E_1E_2)$ complex. Under conditions where the substrate concentration is below saturating, $[S] \ll K_M$, the two catalytic centers will compete for a limiting amount of $S(E_1E_2)$. As shown in Scheme IB, a modifier, M, bound

Scheme I

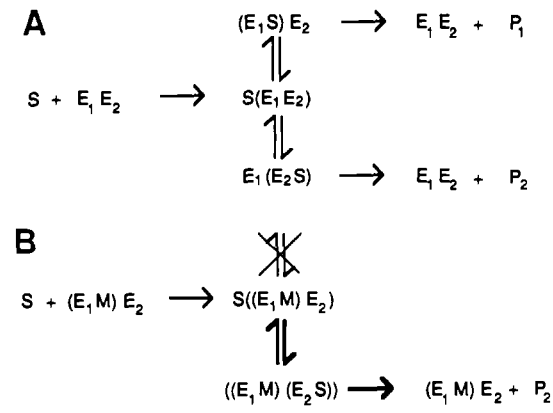

in one catalytic center, for example E_1, will block the transfer of substrate into that catalytic center and passively stimulate the flux of substrate through the other catalytic center by increasing the effective concentration of $S(E_1E_2)$ available for forming $E_1(E_2S)$. The model comprising Scheme IA,B is attractive because it readily explains the observation that the inhibitory and stimulatory effects of the effector molecules leupeptin, and chymostatin are approximately balanced in the early stages of insulin B_{ox} degradation. This is because in the model a competitive inhibitor of one catalytic center is not expected to alter the overall rate of substrate depletion but merely to effect a change in the ratios of products. Studies by Wilk and Orlowski (1983) and Orlowski and Michaud (1989) also indicate that similar effects may be observed with low molecular weight synthetic peptide substrates. Specifically, these investigators have shown that inhibition of the activity that cleaves Z-Gly-Gly-Leu-pNA leads to stimulation of the leupeptin-sensitive trypsinlike activity. Taken together, these observations suggest that the operationally defined activities of this multienzyme complex, which presumably represent two or more structurally distinct types of catalytic center, may operate as a functionally integrated unit for the degradation of polypeptide substrates.

Compartmentation of Intermediates in Protein Degradation. The production of peptide (5–13) from insulin B_{ox} requires cleavage at both the Gln_4–His_5 and the Glu_{13}–Ala_{14} bonds in the same substrate molecule. Cleavage of the Gln_4–His_5 bond was specifically inhibited by leupeptin as well as by three other inhibitors that are presumed to be competitive. Cleavage of the Glu_{13}–Ala_{14} bond was not inhibited by these compounds. It may therefore be concluded that the production of peptide (5–13) requires the concerted action of two different catalytic centers in macropain. The rapid accumulation of peptide (5–13) and the observation that this accumulation does not lag behind the accumulation of the supposed intermediates, peptides (1–13) and (5–30), suggests the hypothesis that the pools of peptides (1–13) and (5–30) in solution are minor sources for production of peptide (5–13) and that intermediates produced by an initial cleavage of a polypeptide substrate in one macropain catalytic center are sometimes channeled to a second catalytic center within the same enzyme complex to be cleaved again. Under this hypothesis, the progress curve for peptide (5–13) (Figure 7) may be interpreted as representing the superposition of at least two pathways, the first in which the products, peptides (5–13), (14–30), and (1–4) are formed via channeled intermediates and the second in which the same products are formed via intermediates that are released into solution and then recaptured. A well-characterized example of this general phenomenon is the chan-

neling of indole in the tryptophan synthase bienzyme complex (Matchett, 1974; Hyde et al., 1988). To account for the absence of a detectable lag in production of peptide (5–13), it is assumed that, at early times of digestion, the peptide (5–13) is produced predominantly from the channeled pathway and that, at later times, after the solution pools of peptides (1–13) and (5–30) accumulate, and the pool of intact insulin B_{ox} is depleted, peptide (5–13) is derived predominantly from the release-and-recapture pathway. At 5 and 10 min, the amount of peptide (5–13) produced was approximately 10% of the total insulin B_{ox} degraded, indicating that 10% of the insulin B_{ox} molecules that are degraded are bound to the enzyme and cleaved in two positions, Gln_4–His_5 and Glu_{13}–Ala_{14}, before release of the resulting products. The identity of the intermediate in the channeling pathway cannot be specified from the data so far obtained, because the products of this pathway, peptides (1–4), (5–13), and (14–30), are expected to accumulate in the same relative amounts regardless of which intermediate, peptide (1–13) or peptide (5–30), is utilized. Thus, the channeling of intermediates between catalytic centers may be either unidirectional or bidirectional and further work will be required to distinguish these possibilities.

The simplest model for such a channeling mechanism would have the two catalytic centers juxtaposed in a microenvironment partially excluded from the bulk solvent. Products of the first cleavage that are released into this microenvironment would more readily diffuse to the second catalytic center than identical molecules present in solution. This hypothesis is consistent with the observation that the rate of production of peptide (5–13) from either peptide (1–13) or peptide (5–30), when supplied directly and in pure form, is much slower than the rate of production of peptide (5–13) from insulin B_{ox} under otherwise identical conditions (L. R. Dick, unpublished observations). In considering more complex possibilities, it is interesting to note that a fully extended polypeptide of 30 amino acid residues (e.g., insulin B_{ox}) spans a distance approximately two-thirds that of the long axis of a macropain particle (Baumeister et al., 1988). A substrate molecule bound to the enzyme could conceivably contact several subunits and be bound in different catalytic centers and allosteric regulatory sites simultaneously. If this occurred, the transit time (the time required for the channeling of an intermediate) would effectively be eliminated and the enzyme might function like a "bread slicer" in which all the cuts are made simultaneously. Furthermore, a competitive inhibitor bound in one catalytic center could affect allosteric regulation by altering the mode of substrate binding to other catalytic centers in the multienzyme complex without necessarily causing conformational changes in the enzyme.

Physiological Role of Channeling in Protein Degradation. Protein synthesis is an example of a metabolic pathway in which the intermediates have no metabolic function other than to become complete proteins (Srere, 1987). We may consider that the bulk of polypeptide intermediates generated during protein degradation also have but one appropriate fate, to be broken down to their constituent amino acids. Our results suggest that macropain can channel polypeptide intermediates in vitro. If the enzyme has this capacity in vivo, the resulting physiological advantages may include, first, an increase in the efficiency of amino acid recycling (Welch, 1977; Gaertner, 1978), and second, a reduction in the pool sizes of polypeptide intermediates that may otherwise tax the limited solvent capacity of the cellular water (Atkinson, 1977).

Acknowledgments

We thank Kevin Kuehn and Harvey Harris for technical support in isolating macropain and J. Royce Potter for secretarial and graphics assistance. We are also grateful to Louis Hersh and Paul Srere for critical reading of the manuscript.

References

Arribas, J., & Castaño, J. G. (1990) *J. Biol. Chem. 265*, 13969–13973.

Atkinson, D. E. (1977) *Cellular Energy Metabolism and Its Regulation*, Academic Press, New York.

Baumeister, W., Dahlmann, B., Hegerl, R., Kopp, F., Kuehn, L., & Pfeifer, G. (1988) *FEBS Lett. 241*, 239–245.

Bradford, M. M. (1976) *Anal. Biochem. 72*, 248–254.

Dahlmann, B., Kuehn, L., Rutschmann, M., & Reinauer, H. (1985a) *Biochem. J. 228*, 161–170.

Dahlmann, B., Rutschmann, M., Kuehn, L., & Reinauer, H. (1985b) *Biochem. J. 228*, 171–177.

Folco, E. J., Busconi, L., Martone, C. B., & Sanchez, J. J. (1988) *Arch. Biochem. Biophys. 267*, 599–605.

Frost, A. A., & Pearson, R. G. (1961) *Kinetics and Mechanism*, 2nd ed., John Wiley & Sons, New York.

Gaertner, F. H. (1978) *Trends Biochem. Sci. 3*, 63–65.

Hyde, C. C., Ahmed, S. A., Padlan, E. A., Miles, E. W., & Davis, D. R. (1988) *J. Biol. Chem. 263*, 17857–17871.

Kuchel, P. W. (1985) in *Organized Multienzyme Systems: Catalytic Properties* (Welch, G. R., Ed.) pp 303–380, Academic Press, Orlando, FL.

Lee, L. W., Moomaw, C. R., Orth, K., McGuire, M. J., DeMartino, G. N., & Slaughter, C. A. (1990) *Biochim. Biophys. Acta 1037*, 178–185.

Mason, R. W. (1990) *Biochem. J. 265*, 479–484.

Matchett, W. H. (1974) *J. Biol. Chem. 249*, 4041–4049.

McGuire, M. J., & DeMartino, G. N. (1986) *Biochim. Biophys. Acta 873*, 279–289.

McGuire, M. J., & DeMartino, G. N. (1989) *Biochem. Biophys. Res. Commun. 160*, 911–916.

McGuire, M. J., McCullough, M. L., Croall, D. E., & DeMartino, G. N. (1989) *Biochim. Biophys. Acta 995*, 181–186.

Orlowski, M., & Michaud, C. (1989) *Biochemistry 28*, 9270–9278.

Rivett, A. J. (1985) *J. Biol. Chem. 260*, 12600–12606.

Rivett, A. J. (1989a) *Arch. Biochem. Biophys. 268*, 1–8.

Rivett, A. J. (1989b) *J. Biol. Chem. 264*, 12215–12219.

Saitoh, Y., Yokosawa, H., Takahashi, K., & Ishii, S. (1989) *J. Biochem. (Tokyo) 105*, 254–260.

Srere, P. A. (1987) *Annu. Rev. Biochem. 56*, 89–124.

Tanaka, K., Ii, K., Ichihara, A., Waxman, L., & Goldberg, A. L. (1986) *J. Biol. Chem. 261*, 15197–15203.

Tanaka, K., Yoshimura, T., Kumatori, A., Ichihara, A., Ikai, A., Nishigai, M., Kameyama, K., & Takagi, T. (1988) *J. Biol. Chem. 263*, 16209–16217.

Tanaka, K., Yoshimura, T., & Ichihara, A. (1989) *J. Biochem. (Tokyo) 106*, 495–500.

Welch, G. R. (1977) *Prog. Biophys. Mol. Biol. 32*, 103–191.

Wilk, S., & Orlowski, M. (1983) *J. Neurochem. 40*, 842–849.

Zolfaghari, R., Baker, C. R. F., Amirgholami, P. C., Canizaro, P. C., & Behal, F. J. (1987) *Arch. Biochem. Biophys. 258*, 42–50.